

# ESTABLISHING SEISMIC SITE CLASS FOR 4 RECORDING STATIONS IN UTTARAKHAND BASED ON GENERALIZED INVERSION AND 1-D EQUIVALENT LINEAR SITE SPECIFIC RESPONSE ANALYSIS

Harinarayan NH<sup>[1]</sup>, Joy Kumar Mondal<sup>[2]</sup>, Abhishek Kumar<sup>[3]</sup>

<sup>1</sup> Research scholar, Indian Institute of Technology, Guwahati – 781039, email:  
n.harinarayan@iitg.ac.in

<sup>2</sup> Research scholar, Indian Institute of Technology, Guwahati – 781039, email:  
joy.mondal@iitg.ac.in

<sup>3</sup> Associate Professor, Indian Institute of Technology, Guwahati – 781039, email:  
abhiak@iitg.ac.in

**Abstract.** In order to understand the current seismicity in different parts of seismicity active regions of India, more than 300 state of the art strong motion recording stations are installed. The ground motion records from these recording stations are available in PESMOS website. Currently PESMOS database is a significant source of ground motion records in India. A serious drawback of PESMOS database is that the recording stations are classified based on the physical description of local geology following Seismotectonic Atlas of India SEISAT (2000) and not based on in-situ field tests. Earlier studies have highlighted ambiguity in the site class (SC) assigned by PESMOS for these recording stations. Accurate assessment of SC of recording stations is essential in order to fully utilize the PESMOS database for regional seismic hazard studies. Several research efforts have been directed towards the use of generalized inversion (GINV) technique as a tool to estimate the local site condition. There is general agreement among the scientific community with regards to the peak frequency ( $f_{\text{peak}}$ ) obtained from the GINV method to identify the soil fundamental frequency. In this study, SC (based on NEHRP classification scheme) of 4 recording stations, located in the region of Uttarakhand, India which are part of PESMOS database, are established using GINV method. In addition, the obtained SCs are compared based on outcomes from 1-D equivalent linear site specific response analysis. The value of  $f_{\text{peak}}$  obtained from above mentioned methods show 1:1 matching.

**Keywords:** Site Class; Generalized Inversion Technique; 1-D equivalent linear site specific response.

## 1 Introduction

Earthquakes (EQs) and EQ related damages are catastrophic in nature. While, most of the losses to life and properties during an EQ are due to falling object and collapsing structures, induced effects of EQ, such as landslides and liquefaction are also common (Kumar et al 2016). EQs cannot be predicted, however, if the damage scenario for an impending EQ can be estimated in advance, suitable modifications in design considerations can be made. The damage pattern during an EQ is proportional to the ground level shaking (peak ground acceleration or PGA). Further, ground level shaking is a function of source, path and site. The bedrock level shaking (peak horizontal acceleration or PHA) can be estimated by performing seismic hazard analysis (SHA) where source (magnitude, fault mechanism, stress drop etc.) and path (anelastic attenuation and geometric spreading) are taken into consideration. In addition, the site effect (local site effects or LSE) also should be considered for analysis. According to Anbazhagan et al (2010), most of EQ damages are attributed to LSE only. Apart from this, there are several instances available where damages due to LSE were reported at hundreds of km away from the epicentre as well (Kumar et al 2015). Effect of LSE on EQ damages were well documented during the 1985 Michoacán EQ (Campillo et al 1989), 1989 Loma Prieta EQ (Chin and Aki 1991), 2011 Sendai EQ (Nihon 2011). In India also, during the 2011 Bhuj EQ, 1999 Chamoli EQ and 2011 Sikkim EQ damages due to LSE have been reported (Mahajan and Viridi 2001, Jain et al 1999, Kumar et al 2016).

The Himalayan mountain range with an approximate length of 2500 km, stretching from Kashmir to Arunachal Pradesh is formed as result of collision of the Indian plate against the Eurasian plate, about 50 million years ago (Gansser 1964). The collision resulted in the formation of a series of faults and thrust zones in this region (Mugnier et al. 2011). The continuing convergence of the Indian plate against the Eurasian plate at an approximate rate of 22 mm/year (Stevens and Avouac, 2016) is the reason for high levels of seismicity of the Himalayan arc. The region has encountered several damage inducing EQs in the past 120 years like the 1905 Kangra EQ ( $M_w = 7.9$ ), the 1934 Bihar-Nepal earthquake ( $M_w = 8.0$ ), the 1950 Assam EQ ( $M_w = 8.6$ ), the 2005 Kashmir EQ ( $M_w = 7.6$ ), the 2011 Sikkim EQ ( $M_w = 6.9$ ) and the 2015 Gorkha and Dholakha EQ ( $M_w = 7.8$  &  $M_w = 7.3$ ). The Himalayan region and its foothills are one among the most densely populated regions in the world and therefore performing seismic hazard studies of this region is very important.

The Government of India installed more than 300 state of the art recording stations consisting of AC-63 GeoSIG triaxial force balanced accelerometers and GSR-18 GeoSIG 18 bit digitizers with external GPS (Kumar et al. 2012) in several seismically active regions with in India to study the ongoing seismicity of the region. EQ records from these recording stations since 2004 are maintained by PESMOS (Program for Excellence in Strong Motion Studies) and are available in the website ([www.pesmos.in](http://www.pesmos.in)). A shortcoming of PESMOS database is the inconsistencies in SC for the recording stations. The recording stations are classified broadly as rock site or soil site based on the physical description of local geology and not based on in-situ field test results. The average shear wave velocity for 30m depth ( $V_{s30}$ ) for each

recording station is approximated based on the SEISAT (2000) and Geological Maps of India. SC for the recording station in PESMOS is given in accordance with the Borchardt (1994) classification scheme. The system consists of 3 SCs namely: SC A ( $V_{s30} > 700\text{m/s}$ ) referring to firm/hard rock site, SC B ( $375\text{m/s} < V_{s30} < 700\text{m/s}$ ) referring to soft to firm rock, and SC C ( $V_{s30} < 375\text{m/s}$ ) referring to soil sites (Mittal et al.2012). In-situ filed studies conducted on some of the recording stations for Uttarakhand region by Pandey et al. (2016) confirmed inconsistencies in the SCs given by PESMOS and field study results. Therefore, ground motion records from PESMOS maintained recording stations cannot be used for seismic hazard studies considering the SC given by PESMOS. In the present study, SC of 4 ground motion recording stations in the Uttarakhand region are estimated using generalized inversion (GNIV) method. Further, one dimensional equivalent linear GRA (ELGRA) are carried out on these 4 stations. Results in the form of site predominant frequency of transfer function ( $f_{\text{peak}}$ ) are estimated. The  $f_{\text{peak}}$  values are also indicative of SCs. Finally the outcome from GNIV and ELGRA are compared.

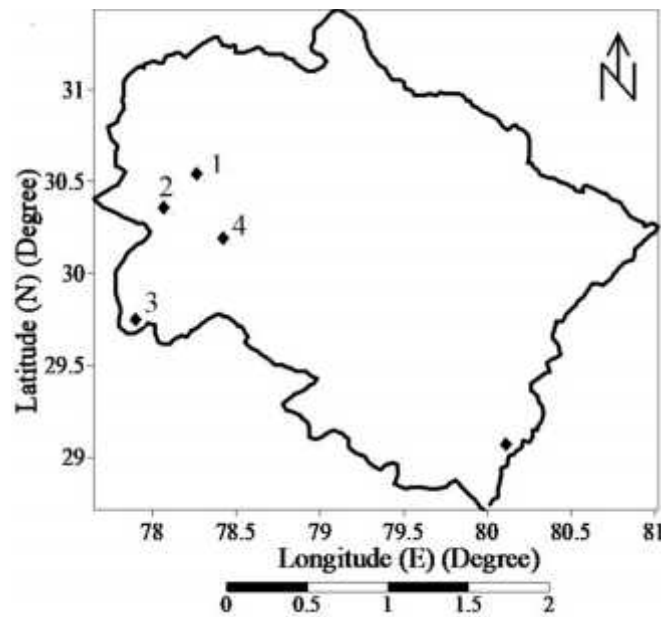


**Fig. 1.** Study area showing 4 recording stations in the state of Uttarakhand considered for the present work (1-Rishikesh; 2- Dehradun, 3-Roorkee and 4-Vikas Nagar)

## 2 Study Area

In the present work, strong motion recording stations at Dehradun, Vikas Nagar, Rishikesh and Roorkee (see Fig. 1) are considered for analyses. The coordinates of

four stations considered in the present study are enlisted in Table 1. Major tectonic feature in the study area includes the Main Central Thrust (MCT) and the Main Boundary Thrust (MBT) (Valdiya 1980). Exploring past seismicity indicates that the region has recently experienced two moderate EQs, namely: 1991 Uttarakashi EQ (Mw=6.8) and 1999 Chamoli EQ (Mw=6.6). These EQs have inflicted severe damages to infrastructure (Verma et al. 2014). Therefore this region could incur heavy loss of life and property during future EQs as well.

**Table 1.** Location Details and  $f_{\text{peak}}$  values of 4 recording stations

| Site       | Lat( $^{\circ}$ ) | Long( $^{\circ}$ ) | $f_{\text{peak}}$ (Hz) |             |             | $V_{s30}$<br>(m/s) | NEHRP<br>SCs |             |
|------------|-------------------|--------------------|------------------------|-------------|-------------|--------------------|--------------|-------------|
|            |                   |                    | GNIV                   | ELGRA       |             |                    |              |             |
|            |                   |                    |                        | Motion<br>1 | Motion<br>2 |                    |              | Motion<br>3 |
| 1          | 2                 | 3                  | 4                      | 5           | 6           | 7                  | 8            | 9           |
| Dehradun   | 30.32             | 78.04              | 2.5                    | 2.41        | 2.51        | 2.4                | 294.6        | D           |
| Vikasnagar | 30.45             | 77.75              | 3.6                    | 3.83        | 3.97        | 3.99               | 461.7        | C           |
| Roorkee    | 29.87             | 77.99              | 1.6                    | 1.83        | 1.78        | 1.77               | 209.4        | D           |
| Rishikesh  | 30.12             | 78.28              | 3.2                    | 2.46        | 2.56        | 2.45               | 320.1        | D           |

### 3 Dataset and processing

The database used in the present study consists of 13 accelerograms recorded during 4 EQs with magnitude in the range 3.9 to 4.6. Details of the EQ are summarized in Table 2. Further, the ground motion records are corrected for baseline (Kumar et al. 2012) and a band pass filter between the frequency range 0.15Hz and 15.0Hz using a Butterworth filter. Afterwards, the S-wave component of the accelerogram is separated similar to Bindi et al., (2009) and the Fourier amplitude spectra is calculated for each EQ record.

**Table 2.** Details of EQs

| Sr. no. | Date       | Lat. | Long | Mag. | Depth (km) |
|---------|------------|------|------|------|------------|
| 1       | 15-05-2009 | 30.5 | 79.3 | 4.1  | 15         |
| 2       | 11-01-2010 | 29.7 | 80   | 3.9  | 15         |
| 3       | 14-03-2010 | 31.7 | 76.1 | 4.6  | 29         |
| 4       | 01-05-2010 | 29.9 | 80.1 | 4.6  | 10         |

### 3.1 GNIV Technique

Andrews (1986) developed GNIV modifying Standard spectral ratio method of Borchardt (1970). Several forms of GNIV have been developed and used for estimating the EQ parameters by various researchers (For e.g. Castro et al. 1990; Boatwright et al. 1991; Oth et al. 2008 etc.). Methodology used in the present study for estimating site characteristics is discussed below.

#### Methodology

The spectral acceleration of the  $i^{th}$  EQ recorded at the  $j^{th}$  recording station ( $A(f)_{ij}$ ) is linearly represented as;

$$\ln A(f)_{ij} = \ln U(f)_i + \ln P(f)_{ij} + \ln G(f)_f \quad (1)$$

In eq. 1,  $U(f)_i$  represents the source effect,  $P(f)_{ij}$  represents the path attenuation term, and  $G(f)_f$  represents the site effect. The path attenuation term is removed from the spectral content of the record in accordance with Andrews 1986 as;

$$\ln A(f)_{ij} - \ln P(f)_{ij} = \ln J(f)_{ij} \quad (2)$$

The value of  $P(f)_{ij}$  in eq. 2 is computed using eq. 3.

$$P(f)_{ij} = \frac{1}{R_{ij}} \left[ e^{\frac{-(\pi f R_{ij})}{Q_s(f)\beta}} \right] \quad (3)$$

In eq. 3,  $R$  represents the hypocentral distance,  $Q_s(f)$  represents the quality factor for S wave (taken as  $Q_s = (105)f^{(0.94)}$  for the study area after Harinarayan and Kumar, 2019a),  $\beta$  represents the average shear wave velocity of the crustal medium for the region (taken as 3.5km/s for the study area after Mukhopadhyay and Kayal, 2003).

The corrected spectra ( $\ln J(f)_{ij}$ ) is substituted in eq. 1 giving:

$$\ln J(f)_{ij} = \ln U(f)_i + \ln G(f)_f \quad (4)$$

The matrix form of eq. 4 is given below.

$$\begin{bmatrix} D \\ C \end{bmatrix} m = \begin{bmatrix} T \\ 0 \end{bmatrix} \quad (5)$$

In eq. 5,  $m$  represents a space matrix containing only two non-zero elements in each row and column which relates to  $\ln U(f)_i$  and  $\ln G(f)_f$  terms.  $D$  in eq. 5 is the matrix linear operator and  $t$  is the data vector containing the elements related to

In  $J(f)_{ij}$  - A row matrix  $C$  is added for the reference station in which  $C \times m = 0$ . The solution for eq. 4 is computed using singular value decomposition method (Menke 1989). In the present work, Pithoragarh station is selected as a reference site based on the findings of Harinarayan and Kumar, (2018a).

### 3.2 Input parameters used in ELGRA methodology

In addition to the method described earlier, the SCs can also be obtained from theoretical transfer function (or Fourier amplification ratio/ F.A.R.) of the site (Harinarayan and Kumar 2018 a,b; Zhao et al 2006). For this, the site natural frequency (or predominant frequency of F.A.R.) has to be determined from theoretical transfer function (Chang et al 1996, Ghyamghamian and Kawakami 1996, Phanikanth et al 2010). Further, it is also highlighted by several studies (Chang et al 1996, Ghyamghamian and Kawakami 1996, Field et al 1997, Ghyamghamian and Motosaka 2001, Ren et al 2017, Wang et al 2019) that during strong EQs, nonlinear soil behavior regulates the ground response and due to decreased shear modulus ( $G$ ), site natural frequency tends to shift toward the lower values. F.A.R. is a direct representation of LSE in the frequency domain, through which relative amplification or deamplification between the bedrock and surface motion can be represented. F.A.R. can be determined by performing equivalent linear ground response analysis (ELGRA). In ELGRA, an important input parameter is ground motion or bedrock motion. Ideally, regionally recorded bedrock ground motions should be considered for performing GRA. However, due to unavailability of such recorded bedrock motions on a regional scale, standard ground motions (eg. 1999 Chi Chi, 1995 Kobe, 1994 Northridge etc.), which are recorded on global level are being considered for GRA (Kumar et al. 2016). In the context of the present study, which focuses on determining SCs, ground motion should be selected in a way that they do not introduce nonlinear soil behavior. Otherwise, the values obtained for site natural frequency may lead to misleading SCs. Earlier, Rubinstein (2011) pointed out that ground motions with PHA as small as 0.035g caused nonlinear soil behavior in Turkey flat array. Similarly, Wu et al (2010) found PHA value of 0.02 induced significant nonlinearity at a site located in Japan. Ghofrani et al (2013) found that threshold PHA values, ranging from 0.004 to 0.15g for 49 sites showed nonlinearity in soil behavior. These studies clearly highlight that even for small level of PHA values, soil can exhibit nonlinearity. Further, it has to be mentioned here, that for low shear strain levels (<0.1-0.3% as per Wang et al 2019) ELGRA can provide reasonable results. Thus, to obtain reasonable values of site natural frequency, 3 weak ground motions are selected from SHAKE2000 database in order to perform ELGRA. The details of the ground motions are shown in Table 3. It can be observed from Table 3, that, the PHA values of the 3 motions are 0.036, 0.009 and 0.008g respectively. These 3 bedrock motions are applied to each of the four sites as bedrock motions. All the ELGRA are performed using the MATLAB code developed by Kumar and Mondal (2017). It has to be highlighted here that the dynamic soil property curves ( $G/G_{max}$  and damping  $\gamma$ ) are also prerequisite for performing ELGRA. Near surface lithology for the 4 sites considered here consisted of soil types such as clay, silty sand, sand and boulders

(Pandey et al 2016). The soil types are modeled in the MATLAB code with standard G/Gmax and  $\gamma$  curves that are widely available in the literature. The silty sand and sand layers are modeled based on G/Gmax and  $\gamma$  curves formulated by Seed and Idriss (1970) for average sand. Similarly, clay soils are modeled as per G/Gmax and  $\gamma$  curves taken from Seed and Idriss (1970) for clay (upper bound). The boulder layers are modeled with G/Gmax and  $\gamma$  curves developed for gravel by Seed et al (1986). Total 12 ELGRA are carried out and results are obtained in the form of F.A.R. between bottom of the borehole and surface.

**Table 3.** Details of ground motions used for ELGRA

| Sr. No. | Ground Motion Details as per SHAKE2000                  | PGA (g) | Duration (s) | Predominant Frequency (Hz) |
|---------|---|---------|--------------|----------------------------|
| 1       | ANCHORAGE, ALASKA 1875, M-6, R81-GOULE HALL STATION     | 0.036   | 18.59        | 5.42                       |
| 2       | BORREGO MOUNTAIN 04/09/68 0230, PASADENA-ATHENAEUM, 270 | 0.009   | 60.23        | 0.61                       |
| 3       | BORREGO MOUNTAIN 04/09/68 0230, TERMINAL ISLAND, 339    | 0.008   | 51.8         | 2.5                        |

#### 4 Result and Discussion

Figs. 2-5 show the horizontal to vertical ratio curves estimated using GINV as well as F.A.R estimated from ELGRA for the stations considered in the present study. It can be observed from Figs. 2-5, that all the curves have distinct peaks at a particular frequency. The frequency corresponding to the first peak of F.A.R (denoted by  $F.A.R_{peak}$ ) is termed as  $f_{peak}$ . The  $f_{peak}$  value represents the natural frequency of the 30m soil column (Phanikanth et al 2010). It can be conceived from Figs. 2-5 that,  $f_{peak}$  values from GINV and ELGRA for respective sites show 1:1 correspondence. However,  $F.A.R_{peak}$  obtained from ELGRA ( $F.A.R_{peak}$ ) and GINV showed significant differences. In the present study,  $F.A.R_{peak}$  values obtained from ELGRA are found to be higher than GINV.

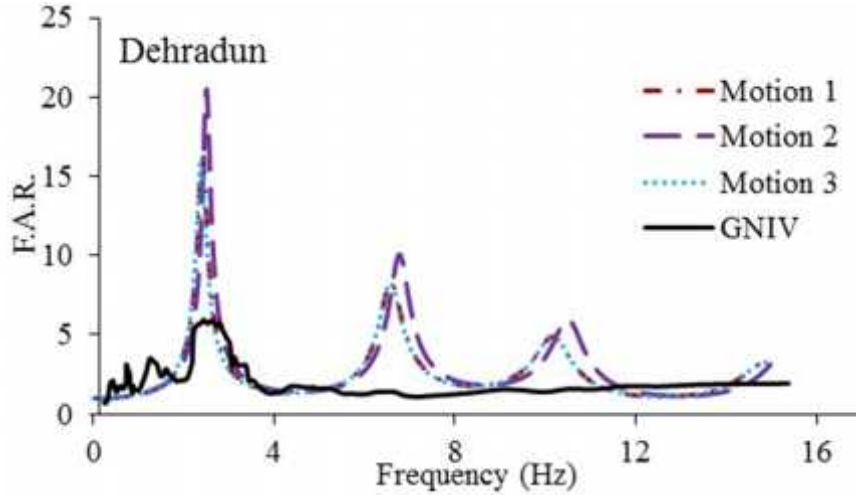


Fig. 2. Comparison of GNIV and ELGRA

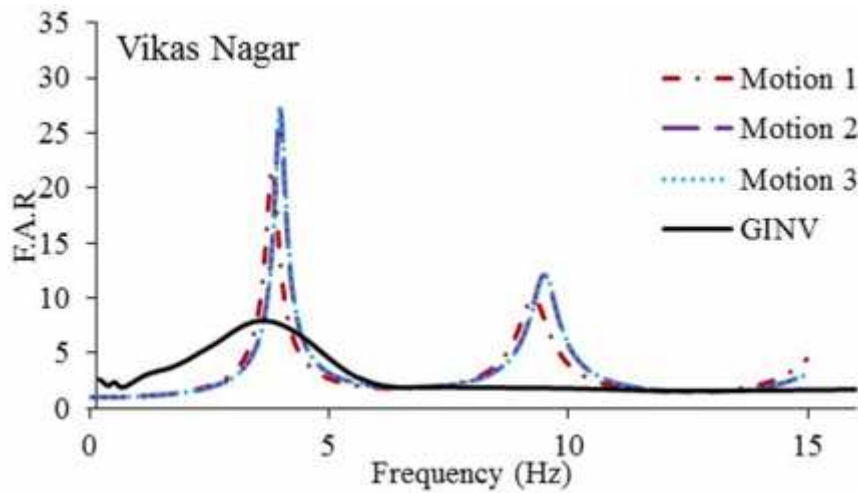


Fig. 3. Comparison of GNIV and ELGRA

It has to be highlighted here that the differences in amplitude values obtained from GNIV and ELGRA have no influence on the determination of SC. This is attributed to the fact that, present study utilizes only the  $f_{\text{peak}}$  values for the identification of SCs. The values of  $f_{\text{peak}}$  obtained based on GNIV and ELGRA are given in Table 1. The values of  $f_{\text{peak}}$  for Dehradun and Vikashnagar recording stations obtained from both GNIV and ELGRA are in the range 2.4-2.51Hz and 3.6-3.99Hz respectively, whereas for Roorkee and Rishikesh values are 1.6-1.8Hz and 2.4-3.2Hz respectively.

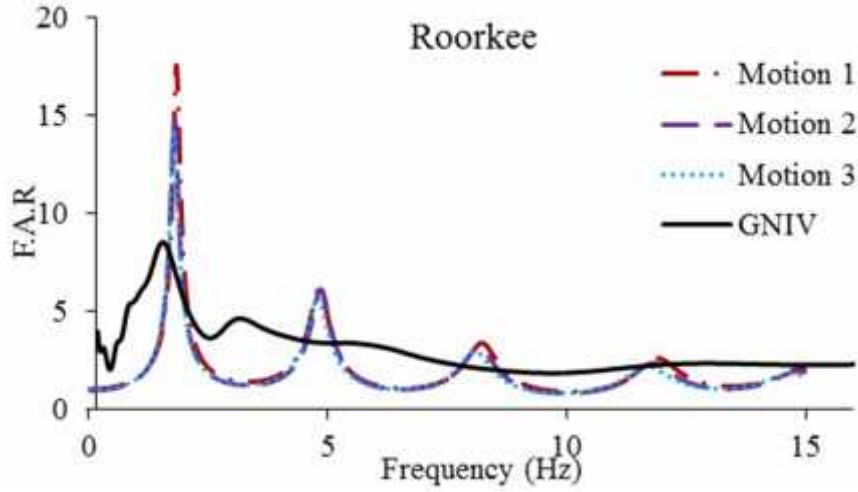


Fig. 4. Comparison of GNIV and ELGRA

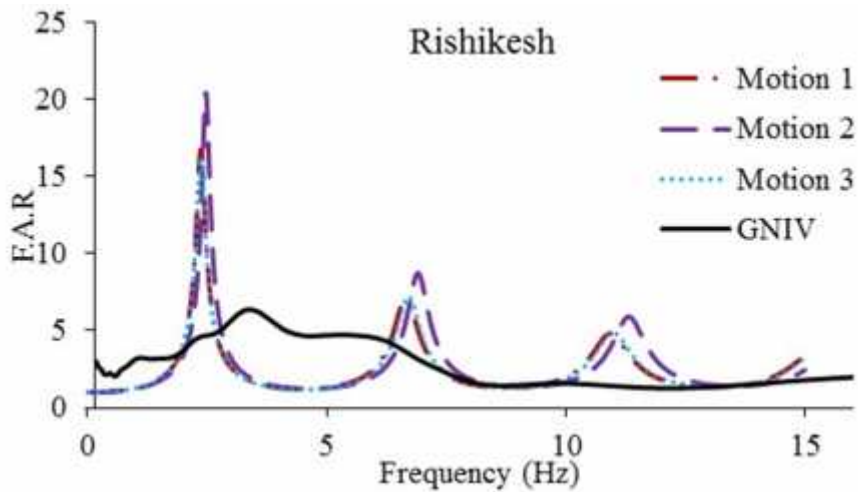


Fig. 5. Comparison of GNIV and ELGRA

As mentioned earlier, accurate site classification of recording stations is important for proper utilization of ground motion records for seismic hazard studies. Site classification of the recording stations considered in the present study is carried out based on the values of  $f_{\text{peak}}$  obtained in the present study. Based on the average value of  $f_{\text{peak}}$  obtained using the two methods, corresponding value of  $V_{s30}$  (shear wave velocity at 30m depth) is calculated using eq. 6 in accordance with Kramer, (1996), for a single layer model over half space considering soil depth as  $H$  (taken as 30m).

$$V_z = f_{\text{peak}} 4H \quad (6)$$

**Table 4.** NEHRP site classification provisions

| Site Class | General description           | Shear wave velocity  |
|------------|-------------------------------|----------------------|
| A          | Hard rock                     | >1500 m/sec          |
| B          | Rock                          | 760 m/sec-1500 m/sec |
| C          | Very dense soil and soft rock | 360 m/sec-760 m/sec  |
| D          | Stiff soil                    | 180 m/sec-360 m/sec  |
| E          | Soft soil                     | <180 m/sec           |

The calculated  $V_{s30}$  values (tabulated Table 1) is utilized to classify the recording stations as per widely used NEHRP classification scheme (shown in Table 4). Based on the present study Dehradun, Roorkee and Rishikesh belong to SC D whereas, Vikashnagar belongs to SC C.

## 5 Conclusion

In the present work, SCs of 4 recording stations located in the Uttarakhand region are established based on results obtained from GNIV and ELGRA. The F.A.R curves obtained using GINV and ELGRA exhibit identical  $f_{peak}$  values. Further,  $V_{s30}$  values are computed based on  $f_{peak}$  values obtained in the present study and NEHRP based site classification is attempted. It has been found that, Vikashnagar belongs to SC C and Dehradun, Roorkee and Rishikesh belong to SC D. Outcome of the present work is very helpful for the use of ground motion records from the recording stations considered in the present work, for surface seismic hazard studies.

## References

1. Anbazhagan, P., Ththingbaijam, K.K.S., Nath, S.K., Kumar, J.N., Sitharam, T.G.: Multi-criteria seismic hazard evaluation for Bangalore city, India. *Journ. of Asian earth Sci* 38(5), 186-198 (2010)
2. Andrews, D. J.: Objective determination of source parameters and similarity of earthquakes of different size, *Earthquake source mechanics*, 259-267 (1986).
3. Bindi, D., Pacor, F., Luzi, L., Massa, M., Ameri, G.: The Mw 6.3, 2009 L'Aquila earthquake: source, path and site effects from spectral analysis of strong motion data, *Geophys. J. Int.*, 179(3), 1573-1579 (2009)
4. Boatwright, J., Fletcher, J.B., Fumal, T.E.: A general inversion scheme for source, site, and propagation characteristics using multiply recorded sets of moderate-sized earthquakes, *Bull. Seism. Soc. Am.*, 81(5), 1754-1782 (1991).
5. Borchardt, R. D.: Effects of local geology on ground motion near San Francisco Bay, *Bull. Seism. Soc. Am.*, 60, 29-61 (1970)
6. Borchardt, R.D.: Estimates of Site-Dependent Response Spectra for Design (Methodology and Justification), *Earthq. Spectra*, 10, 617-653 (1994)

7. Campillo, M., Gariel, J.C., Aki, K., Sanchez-Sesma, F.J.: Destructive strong ground motion in Mexico City: Source, path and site effects during great 1985 Michoacan earthquake. *Bull of Seismol Soc. of America* 79, 1718-1735 (1989)
8. Castro, R. R., Anderson, J. G., Singh, S. K.: Site response, attenuation and source spectra of S waves along the Guerrero, Mexico, subduction zone, *Bull. Seismol. Soc. Am.*, 80(6A), 1481-1503 (1990)
9. Chang, C.Y., Mok, C.M., members, ASCE, Tang, H.T: Interference of dynamic shear modulus from Lotung downhole data. *Journ of Geotech Engg* 122(8), 657-665 (1996)
10. Chin, B., Aki, K.: Simultaneous study of the source, path and site effects on strong ground motion during the 1989 Loma Prieta earthquake: A preliminary result on pervasive nonlinear site effects. *Bull of Seismol Soc of America* 81, 1859-1884 (1991)
11. Field, E. H., Jacob, K. H.: A comparison and test of various site-response estimation techniques, including three that are not reference-site dependent, *Bull. Seismol. Soc. Am.*, 85(4), 1127-1143 (1995)
12. Field, E.H., Johnson, P.A., Berensev, I.A., Zeng, Y.: Nonlinear ground-motion amplification by sediments during the 1994 Northridge earthquake. *Nature* 390(6660), 599 (1997)
13. Gansser, A.: *Geology of the Himalaya*, Interscience, New York, 289 (1964).
14. Ghayamghamian, M., Matosaka, M.: Identification of dynamic soil properties using vertical array recordings. *Proc. Int. Conf. on Recent Advances in Geotech. Earthq. Eng. and Soil Dyn.* Paper no 22. (2001)
15. Ghayamghamian, M.R., Kawakami, H.: On the characteristics of non-linear soil response and dynamic soil properties using vertical array data in Japan. *Earthq and Struct Dyn* 25, 857-870 (1996)
16. Ghofrani, H., Atkinson, G.M., Goda, K.: Implications of the 2011 M9.0 Tohoku Japan earthquake for the treatment of site effects in large earthquakes. *Bull of Earthq Engg* 11(1), 171-203 (2013)
17. Harinarayan, N. H., Kumar A.: Estimation of path attenuation and site characteristics in the north-west Himalaya and its adjoining area using generalized inversion method, *Annals of Geophysics*. (Under review) (2019a).
18. Harinarayan, N. H., Kumar, A.: Determination of NEHRP Site Class of Seismic Recording Stations in the Northwest Himalayas and Its Adjoining Area Using HVSR Method, *Pure Appl. Geophys.*, 175(1), 89-107(2018a).
19. Harinarayan, N. H., Kumar, A.: Seismic Site Classification of Recording Stations in Tarai Region of Uttarakhand, from Multiple Approaches, *Geot. Geol. Eng.*, 1-16(2018b).
20. Harinarayan, N. H., Kumar, A.: Estimation of source and site characteristics in the North-West Himalaya and its adjoining area using generalized inversion method. *Annals of Geophysics*, 62, 8. (2019b).
21. Jain, S.K., Murthy, C.V.R., Jaswant, N.A., Rajendran, C.P., Rajendran, K., Sinha, R.: Chamoli (Himalaya, India) earthquake of Mrch 1999. *EERI special report* 33 (7)
22. Kakkamanos, J., Baise, L.G., Thompson, E.M., Dorfmann, L.: Comparison of 1D linear, equivalent-linear, and nonlinear site response models at six Kik-net validation sites. *Sol Dyn and Earthquake Engg* 69, 207-219 (2015)
23. Kumar, A., Baro, O., Harinarayan, N.H.: Obtaining the surface PGA from site response analysis based on globally recorded ground motions and matching with codal values. *Nat Hazards* 81, 543-572 (2016).
24. Kumar, A., Mittal, H., Sachdeva, R., Kumar, A.: Indian strong motion instrumentation network, *Seismol. Res. Lett.*, 83(1), 59-66 (2012)

25. Kumar, A., Mondal, J. K.: Newly developed MATLAB based code for equivalent linear site response analysis. *Geotechnical and Geological Engineering*, 35, 2303–2325 (2017)
26. Mahajan, A.K., Viridi, K.S.: Macro seismic field generated by 29 March, 1999 Chamoli earthquake and Seismotectonics. *Journ Asian earth Sci* 19(4), 507-516 (2001)
27. Menke, W.: *Geophysical data analysis: Discrete inverse theory*. Academic press. (2018).
28. Mugnier, J.L., Gajurel, A., Huyghe, P., Jayangondaperumal, R., Jouanne, F., Upreti, B.: Structural interpretation of the great earthquakes of the last millennium in the central Himalaya. *Earth Sci Rev* 127: 30-47 (2013)
29. Nihon: Liquefaction induced damages caused by the M 9.0 east Japan mega earthquake on March 2011, Tokyo Metropolitan University, Hisataka Tano, Nihon University, Koriyama Japan, with cooperation of save Earth co. and Waseda University. (2011)
30. Oth, A., Bindi, D., Parolai, S., Wenzel F.: S-wave attenuation characteristics beneath the Vrancea region in Romania: new insights from the inversion of ground-motion spectra, *Bull. Seism. Soc. Am.*, 98(5), 2482-2497(2008).
31. Pandey, B., Jakka, R.S., Kumar, A.: Influence of local site conditions on strong ground motion characteristics at Tarai region of Uttarakhand, India. *Nat Hazards* 81: 1073-1089 (2016)
32. Phanikant, V.S., Choudhury, D., Reddy, G.R. : Equivalent-linear seismic ground response analysis of some typical sites in Mumbai, *GeotechGeolEng* 29, 1109-1126 (2011)
33. Ren, Y., Wen, R., Yao, X., Ji, K.: Five parameters for the evaluation of the soil nonlinearity during the M<sub>s</sub> 8.0 Wenchuan Earthquake using HVSR method. *Earth Planets Space* 69(1), 116 (2017)
34. Rubinstein, J.L.: Nonlinear site response in medium magnitude earthquakes near Parkfield, California. *Bull of Seismol Soc of America* 101(1), 275-286 (2011)
35. Seed, H.B., Idriss, I.M: Soil moduli and damping factors for dynamic response analysis. Report no. EERC 70-10. University of California Berkeley (1970)
36. Seed, H.B., Wong, R.T., Idriss, I.M., Tokimatsu, K.: Moduli and damping factors for dynamic analyses of cohesionless soils. *J GeotechEng, ASCE*, 112(11), 1016-1032 (1986)
37. Stevens, V.L., Avouac, J.-P.: Interseismic coupling on the main Himalayan thrust. *Geophys. Res. Lett.* 42, 5828–5837 (2015)
38. Valdiya, K. S.: Evolution of the Himalaya, *Tectonophysics*, 105(1-4), 229-248 (1984)
39. Wang, H.Y., Jiang, W.P.; Wang, S.Y., Miao, Y.: In situ assessment of soil dynamic parameters for characterizing nonlinear seismic site response using Kik-net vertical array data. *Bull of Earthq Engg* 17, 2331-2360 (2019)
40. Wu, C., Peng, Z., Ben\_Zion, Y: Refined thresholds for non-linear ground motion and temporal changes of site response associated with medium-size earthquakes. *Journ of Geophys* 182(3), 1567-1576 (2010)